Inorganic Chemistry

Article

pubs.acs.org/IC

Anionic Guests in Prismatic Cavities Generated by Enneanuclear Nickel Metallacycles

Jordi Esteban,*[,†] Mercè Font-Bardia,[‡,§] and Albert Escuer*[,†]

[†]Departament de Química Inorgànica, Universitat de Barcelona, Av. Diagonal 645, 08028 Barcelona, Spain

[‡]Departament de Mineralogia, Cristal·lografia i Dipòsits Minerals, Universitat de Barcelona, Martí Franqués s/n, 08028 Barcelona, Spain

[§]Unitat de Difracció de R-X, Centre Científic i Tecnològic de la Universitat de Barcelona (CCiTUB), Universitat de Barcelona, Solé i Sabarís 1-3, 08028 Barcelona, Spain

Supporting Information

ABSTRACT: The combination of polydentate aminated ligands with the 2-pyridyloxime-nickel-azide system leads to series of clusters with unprecedented topologies. Among them, a remarkable family of {Ni_9} metallacycles that are capable of selective encapsulation of azide/halide anions in a cryptand-like cavity through hydrogen-bond interactions has been characterized.

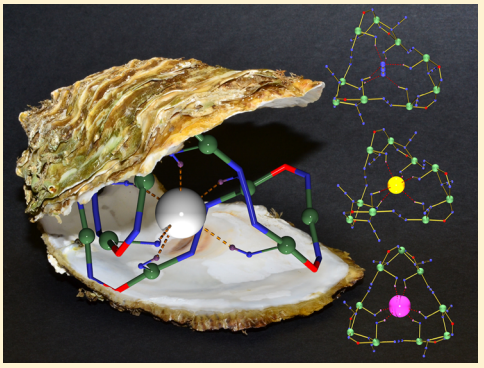

INTRODUCTION

Anion binding and sensing is an expanding field within supramolecular chemistry, because of its applications in anion exchange and transport, biomedical and environmental monitoring, molecular recognition, and crystal engineering.[1] Among the different supramolecular strategies to synthesize this receptors, chemical (anion) template[2] offers a rational and efficient approach to molecular and supramolecular assemblies, but also allows the preparation of unusual topologies, such as rotaxanes, helicates, and catenanes.[3]

Despite the fact that most anion receptors are preformed organic molecules,[2a,4] the number of hosts that incorporate metallic centers in its structure is increasing.[5] Typical functions for metal centers in anion hosts have been structure-organizing and binding groups but, furthermore, the positive charge of the metal center contributes to a more favorable binding via columbic interaction, which is added to other host−guest interactions. One of the most useful noncovalent host−guest interactions are hydrogen bonds, because of their directionality and relative strength. In addition, the presence of nearby electron-withdrawing metal centers can boost the hydrogen-bond donor ability of the group and, consequently, enhance the host−guest interaction.

Coordination of azide anion by the well-known (N_3) ⊂ [BT-6H$^+$] bis-trend hexaprotonated cryptand[6] was established by the Lehn group in his seminal work in 1984. However, after this early work, the number of X-ray characterized specific receptors for this anion is surprisingly reduced in comparison with oxoanions or halides: in addition to the preformed [BT-6H$^+$] cryptand in which the azide anion is linked by six hydrogen bonds in a prismatic arrangement, only five preformed organic receptors[7] and one pseudo-spherical metallocage in which the interaction with the guest involves weak C−H···N bonds,[8] have been recently characterized.

Pyridyloximes have been extensively employed in recent years in cluster coordination chemistry,[9] because of their coordinative versatility, that allows them to bridge up to four metallic centers and their easy functionalization. Focusing on nickel derivatives, the chemistry of 2-pyridyloximes, (py)C{R}-NOH, has yielded a large variety of topologies and nuclearities up to Ni_{14}.[10] Combination of pyridyloximes and μ-1,1-azido bridges has proven an adequate method to obtain high-spin ground states and with SMM response in some cases.[11]

In the search of new synthetic routes, we have combined aliphatic polydentate amines with the nickel−oximato−azido system (Chart 1), and we report the syntheses and characterization (see details and Scheme S1 in the Supporting Information) of the trinuclear complex $[Ni_3(Medpt)_2(py_2CNO)_2(N_3)_4]$ (**1**·MeOH); the tetranuclear compounds $[Ni_4(Medpt)_2(N_3)_4(dapdo)_2]$ (**2**·MeOH), $[Ni_4(dpt)_2(N_3)_4(py_2CNO)_4]$ (**3**·2MeCN), and $[Ni_4(Me_3dpt)_2(N_3)_4(pyC\{ph\}NO)_4]$ (**4**·4MeCN); the pentanuclear complex $[Ni_5(H_2O)_4(AcO)_2(N_3)_2(OH)_2(pyC\{ph\}-$

Received: October 22, 2013
Published: December 30, 2013

   dx.doi.org/10.1021/ic402651k | *Inorg. Chem.* 2014, 53, 1113−1121

Chart 1. Pyridyloximate and Tridentate Aminated Ligands Discussed in the Text

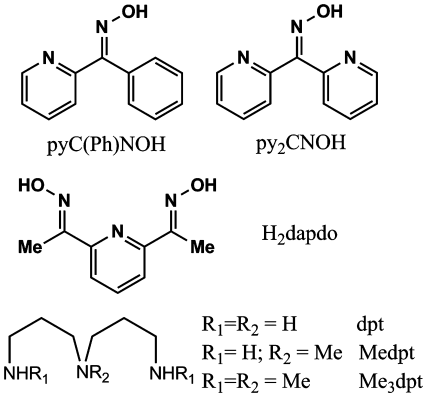

$NO)_4]$ (**5**·5MeCN,H_2O); and a series of enneanuclear metallacycles with formula: $(N_3) \subset [Ni_9(dpt)_6(pyC\{ph\}NO)_6(N_3)_9](A)_2$ (where A = NO_3^- (**6**·MeCN), BF_4^- (**7**·$2H_2O$), F^- (**8**·MeOH), and Cl^- (**9**·H_2O)), $(X) \subset [Ni_9(dpt)_6(pyC\{ph\}NO)_6(N_3)_9](X)_2$ (X = Br^- (**10**·H_2O) and I^- (**11**·$2H_2O$)), and $(N_3) \subset [Ni_9(dpt)_6(py_2CNOH)_6(N_3)_9](ClO_4)_2$ (**12**·2MeOH), in which py_2CNO^-, $pyC\{ph\}NO^-$, and $dapdo^{2-}$ are the deprotonated forms of dipyridylketoneoxime, phenyl-pyridyl-ketoneoxime and 2,6-diacetylpyridinedioxime, respectively, and dpt is dipropyltriamine.

This work focuses on two types of compounds derived from the new synthetic strategy of blending of 2-pyridyloximates with aliphatic amines: (i) the complete description of series of low-nuclearity complexes (Ni_3, Ni_4, and Ni_5); and (ii) the description of unprecedented series of nonanuclear metallacrowns able to coordinate a variety of anions in a similar way to classic cryptands. An exhaustive structural analysis of the $\{Ni_9\}$ family has been carried out, and some comments about the system selectivity are pointed out. Unfortunately, the labile bis-monodentate μ-1,3-azido bridge is broken in solution as was proven by mass spectroscopy,[12] and then these complexes are only stable in solid state, preventing the study of association constants. Finally, DC susceptibility measurements carried in the 2−300 K temperature range have been realized for all the reported topologies. Compounds **1**, **6**, and **9**−**11** were previously described in a short communication.[12]

EXPERIMENTAL SECTION

Syntheses. py_2CNOH and pyC{ph}NOH ligands, as well as the aminated groups, were purchased from Sigma−Aldrich, Inc., and used without further purification. Nickel salts were purchased form Sigma−Aldrich, Inc., Fluka AG, and Strem Chemicals, Inc.

*$[Ni_3(Medpt)_2(py_2CNO)_2(N_3)_4]$·MeOH (**1**).* Compound **1**, which is defined as $[Ni_3(Medpt)_2(py_2CNO)_2(N_3)_4]$·MeOH, was obtained in good yield via reaction in methanolic medium of py_2CNOH ligand (199 mg, 1 mmol), $[Ni_2(Medpt)_2(N_3)_4]$ (576 mg, 1 mmol), and triethylamine (202 mg, 2 mmol). The resulting solution was left to slow evaporation and prismatic dark crystals appeared after a week. Anal. Calcd for $C_{37}H_{58}N_{24}Ni_3O_3$ (**1·MeOH**): C, 41.8%; H, 5.5%; N, 31.6%. Found: C, 40.9%; H, 5.3%; N, 31.5%.

*$[Ni_4(Medpt)_2(N_3)_4(dapdo)_2]$·MeOH (**2**).* Compound **2**, which is defined as $[Ni_4(Medpt)_2(N_3)_4(dapdo)_2]$·MeOH, was obtained from the reaction of $[Ni_2(Medpt)_2(N_3)_4]$ (576 mg, 1 mmol), $dapdoH_2$ ligand (178 mg, 1 mmol) and NEt_3 (202 mg, 2 mmol) in 20 mL of MeOH. The mixture was stirred, filtered, and left for slow crystallization in a closed vial. Red prismatic crystals were collected a month later. Anal. Calcd for $C_{32}H_{56}N_{24}Ni_4O_4$ (**2**): C, 35.7%; H, 5.2%; N, 31.2%. Found: C, 35.2%; H, 5.0%; N, 31.6%.

*$[Ni_4(dpt)_2(N_3)_4(py_2CNO)_4]$·2MeCN (**3**) and $[Ni_4(Me_3dpt)_2(N_3)_4(pyC\{ph\}NO)_4]$·4MeCN (**4**).* Compounds **3** ($[Ni_4(dpt)_2(N_3)_4(py_2CNO)_4]$·2MeCN) and **4** ($[Ni_4(Me_3dpt)_2(N_3)_4(pyC\{ph\}NO)_4]$·4MeCN) were synthesized from $NiCl_2·6H_2O$ (474 mg, 2 mmol), dipropylene triamine (262 mg, 2 mmol) with py_2CNOH (199 mg, 1 mmol); and $Ni(BF_4)_2·6H_2O$ (680 mg, 2 mmol), Me_3dpt (346 mg, 2 mmol) with pyC{ph}NOH (198 mg, 1 mmol), respectively, together with NaN_3 (260 mg, 4 mmol) and NEt_3 (202 mg, 2 mmol) in 20 mL of MeCN. The resultant mixtures were stirred, filtered, and left for slow evaporation. Red prismatic crystals were collected after a month. Anal. Calcd for $C_{56}H_{66}N_{30}Ni_4O_4$ (**3**): C, 46.1%; H, 4.6%; N, 28.8%. Found: C, 45.5%; H, 4.8%; N, 28.3%.

*$[Ni_5(H_2O)_4(AcO)_2(N_3)_2(OH)_2(pyC\{ph\}NO)_4]$·5MeCN,$H_2O$ (**5**).* Compound **5**, which is defined as $[Ni_5(H_2O)_4(AcO)_2(N_3)_2(OH)_2(pyC\{ph\}NO)_4]$·5MeCN,$H_2O$, was obtained as red brick-shaped crystals from the slow evaporation of the resultant solution of $Ni(AcO)_2·4H_2O$ (594 mg, 2 mmol), pyC{ph}NOH (199 mg, 1 mmol), Me_3dpt (346 mg, 2 mmol), NaN_3 (260 mg, 4 mmol), and NEt_3 (202 mg, 2 mmol) in 20 mL of MeCN. Anal. Calcd for $C_{52}H_{52}N_{14}Ni_5O_{14}$ (**5**): C, 46.1%; H, 4.5%; N, 28.8%. Found: C, 43.8%; H, 4.2%; N, 27.1%.

*$(N_3) \subset [Ni_9(dpt)_6(pyC\{ph\}NO)_6(N_3)_9](NO_3)_2$·MeCN (**6**).* Compound **6**, which is defined as $(N_3) \subset [Ni_9(dpt)_6(pyC\{ph\}NO)_6(N_3)_9](NO_3)_2$·MeCN, was synthesized via reaction of pyC{ph}NOH (198 mg, 1 mmol), $Ni(NO_3)_2$ (580 mg, 2 mmol), dipropylene triamine (162 mg, 2 mmol), NaN_3 (260 mg, 4 mmol), and NEt_3 (202 mg, 2 mmol) in 20 mL of acetonitrile. The solution was left to evaporate slowly and brown prisms were obtained after a week. Anal. Calcd for $C_{108}H_{156}N_{62}Ni_9O_{12}$ (**6**): C, 42.6%; H, 5.2%; N, 28.5%. Found: C, 42.4%; H, 5.2%; N, 29.0%.

*$(N_3) \subset [Ni_9(dpt)_6(pyC\{ph\}NO)_6(N_3)_9](A)_2$ (A = BF_4 (**7**), F (**8**), and Cl (**9**); $(X) \subset [Ni_9(dpt)_6(pyC\{ph\}NO)_6(N_3)_9](X)_2·nH_2O$ (X = Br (**10**), I (**11**); and $(N_3) \subset [Ni_9(dpt)_6(py_2CNO)_6(N_3)_9](ClO_4)_2·2MeOH$ (**12**).* Compounds **7**, **8**, and **9** (defined as $(N_3) \subset [Ni_9(dpt)_6(pyC\{ph\}NO)_6(N_3)_9](A)_2$ (where A = BF_4 (**7**), F (**8**), and Cl (**9**)), **10** and **11** (defined as $(X) \subset [Ni_9(dpt)_6(pyC\{ph\}NO)_6(N_3)_9](X)_2·nH_2O$ (where X = Br (**10**) and I (**11**)), and **12** (which is defined as $(N_3) \subset [Ni_9(dpt)_6(py_2CNO)_6(N_3)_9](ClO_4)_2·2MeOH$) were obtained following the same procedure as that for compound **6** in methanolic solution, starting from the corresponding nickel salt and using the py_2CNOH ligand instead of pyC{ph}NOH for **12**. Dark prisms crystallized one week later. Anal. Calcd for $C_{108}H_{160}B_2F_8N_{60}Ni_9O_8$ (**7·2H$_2$O**): C, 41.5%; H, 5.1%; N, 26.8%. Found: C, 37.5%; H, 4.7%; N, 23.7%. Anal. Calcd for $C_{108}H_{158}Cl_2N_{60}Ni_9O_7$ (**9·H$_2$O**): C, 43.1%; H, 5.3%; N, 28.0%. Found: C, 42.3%; H, 5.1%; N, 28.1%. Anal. Calcd for $C_{108}H_{158}Br_3N_{57}Ni_9O_7$ (**10·H$_2$O**): C, 41.4%; H, 5.1%; N, 25.5%. Found: C, 41.5%; H, 5.2%; N, 25.7%. Anal. Calcd for $C_{108}H_{160}I_3N_{57}Ni_9O_8$ (**11·2H$_2$O**): C, 39.4%; H, 4.9%; N, 24.4%. Found: C, 39.8%; H, 5.0%; N, 24.1%. Anal. Calcd for $C_{104}Cl_2H_{154}I_3N_{66}Ni_9O_{16}$ (**12·2MeOH**): C, 38.8%; H, 4.8%; N, 29.2%. Found: C, 39.8%; H, 5.0%; N, 28.1%.

All samples were obtained in good yield (~40%) as well-formed large crystals. The yield of the reactions is greater than 40%, but it was not quantified, because the collection of the samples for instrumental measures was limited to the well-formed first crystalline fraction.

Physical Measurements. Magnetic susceptibility measurements were carried out on polycrystalline samples with a MPMS5 Quantum Design susceptometer working in the range of 30−300 K under an external magnetic field of 0.3 T and under a magnetic field of 0.03 T in the temperature range of 30−2 K, to avoid saturation effects. Diamagnetic corrections were estimated from the Pascal tables. Infrared spectra (4000−400 cm^{-1}) were recorded from KBr pellets on a Bruker IFS-125 FT-IR spectrophotometer.

X-ray Crystallography. Details of crystal data, data collection, and refinement are given in Tables S1, S2, and S3 in the Supporting Information, whereas experimental details for all compounds are provided in Tables S4−S8 and Figures S1−S5 in the Supporting Information. X-ray data were collected on a MAR345 diffractometer with an image plate detector for compounds **1**, **2**, **3**, and **7**, on a Bruker

dx.doi.org/10.1021/ic402651k | Inorg. Chem. 2014, 53, 1113−1121

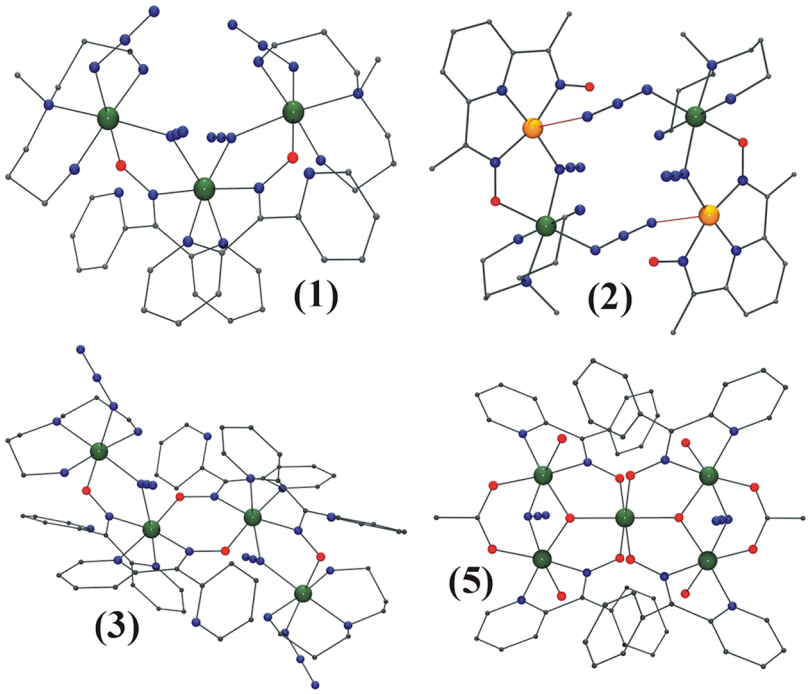

Figure 1. View of the molecular structure of complexes **1**, **2**, **3**, and **5**. The weak axial azido−nickel interaction in compound **2** is depicted in orange color. Color key: O, red; N, blue; C, black; octahedral Ni^{II}, green; and square planar Ni^{II}, orange.

Kappa ApexII CCD diffractometer for compounds **6** and **8**−**12**, on a Supernova ssytem for compound **4**, and on a Bruker D8 Venture system for **5**, with Mo Kα radiation (λ = 0.71073 nm). The structures were solved by direct methods using SHELXS computer program[13] and refined using a full-matrix least-squares method with the SHELXS97 computer program.[14]

All data can be found in the supplementary crystallographic data for this paper in CIF format with CCDC Nos. 859276−859278, 876039−876040, and 948759−948765. These data can be obtained free of charge from The Cambridge Crystallographic Data Centre via www.ccdc.cam.ac.uk/data_request/cif.

Plots for publication were generated with ORTEP3 for Windows and plotted with Pov-Ray programs.[15]

RESULTS AND DISCUSSION

Comments to the Syntheses. Our initial synthetic strategy was to employ, as the nickel source, the neutral dinuclear complex $[Ni_2(Medpt)_2(N_3)_4]$ (previously reported by us[16]), which contains the aminated ligand Medpt and preformed μ-1,1-azido bridges. Our objective was to avoid the presence of counteranions other than azide, in order to reach the syntheses of ferromagnetic clusters containing μ-1,1-azido bridges. As result of the reaction of $[Ni_2(Medpt)_2(N_3)_4]$ with a variety of pyridyloximes (Chart 1), neutral complexes **1** and **2** were characterized.

In light of the structural data, we realized that, despite the presence of terminal azido ligands, the nuclearity of cluster **1** is limited to the low nuclearity Ni_3 entity. This complex is neutral and in order to bind these terminal azido ligands, additional counteranions were needed to balance the resulting positive charge. Thus, the same reaction was tried from $[Ni_2(Medpt)_2(N_3)_4]$ and $[Ni_2(dpt)_2(N_3)_4]$ adding small amounts of sodium nitrate and then, enneanuclear complex **6** was obtained. Further synthetic work revealed that the $\{Ni_9\}$ ring **6** can be obtained in high yield from the direct reaction of nickel nitrate, the aminated ligand, and sodium azide, and the direct synthesis was assumed to be preferable, as described in the Syntheses section for **6**−**12**.

From this result, similar reactions with series of different starting reagents were performed in order to elucidate three questions: (i) the effect of the anion on the final structure, (ii) the influence of the aminated ligand, and (iii) the ability of this system to encapsulate spherical anions as halides.

In addition to the medium nuclearity compounds **3**−**5**, reaction with BF_4^- or ClO_4^- salts gave structures similar to that of the nitrate complex **6** (complexes **7** and **12**). Reaction starting from Ni^{II} halides yields the same structure for fluoride and chloride (**8** and **9**) but successful incorporation of the halide anion as a guest was achieved starting from $NiBr_2$ and NiI_2 salts (complexes **10** and **11**). Complex **5** is the only one that does not incorporate the tridentate amine in its structure, which gives proof of the stability of the bowtie topology[11,17] for the oximato/azide/carboxylato blend of ligands and is closely related to $[Ni_5(MeOH)_4(AcO)_2(N_3)_2(\mu_3\text{-}N_3)_2(pyC\{ph\}NO)_4]$ which contains a μ_3-N_3 ligand instead the μ_3-OH central donor.[11]

Description and Magnetic Study. Plots of the structure of the neutral complexes **1**−**5** are shown in Figure 1. Labeled plots and selected structural parameters are given in Figures S1−S5 and Tables S4−S8 in the Supporting Information.

Compound **1** consists of a neutral angular trinuclear unit linked by double oximato/μ-1,1-azide bridges (Figure 1). The central Ni-atom exhibits a NiN_6 coordination sphere from two py_2CNO^- ligands (each one bound by two of their N atoms) and the two N_3^- binding groups whereas external Ni atoms present a NiN_5O environment that comes from one Medpt ligand, which acts as tridentate ligand in *mer* coordination, one bridging and one terminal azide group and finally an O-oximato ligand. Ni−N−Ni bond angles are relatively large with values of 112.9(1)° and 112.2(1)° and the Ni−O−N-Ni torsion angles are 17.0(3)° and 4.3(3)°.

dx.doi.org/10.1021/ic402651k | *Inorg. Chem.* 2014, 53, 1113−1121

Complex **2** consists of two dinuclear subunits linked by means of μ-1,3-azido bridges. Each subunit is formed by two Ni atoms (one of them linking one tridentate Medpt ligand and the other linking one dapdo^{2-} dioximate), bridged as in the previous complex by a double oximato/μ-1,1-N_3^- bridge, which exhibits similar Ni−N−Ni and Ni−O−N-Ni angles of 112.36(9)° and 14.6(2)°, respectively. The Ni atom linked to the Medpt ligand shows an octahedral environment, whereas the Ni atom coordinated to the dapdo^{2-} ligand exhibits a square planar environment in agreement the high field induced by the fully deprotonated dapdo^{2-} dioximate.[18] Weak Ni−N(azide) interaction with bond distance of 2.820(3) Å (Figure 1) and a set of hydrogen bonds link the two subunits to give the tetranuclear system (see details given in Figure S2 in the Supporting Information).

A view of the core of compound **3** is illustrated in Figure 1. The centrosymmetric tetranuclear complex **3** can be described as being similar to two oximato/μ-1,1-N_3^- bridged dinuclear subunits (similar to compound **1**), linked together by a double oximato bridge. As in the previous case, the central Ni atoms are coordinated by the N atoms of the pyridyloximate ligands, whereas the peripheral nickels bind the aminated tridentate ligands. Ni−N−Ni bond angle is 111.4(1)° and Ni−O−N−Ni torsion angles are 20.0(2)° and 24.0(2)°. The different ligands employed in **3** (Medpt and py_2CNO^-) and **4** (Me_3dpt and pyC{ph}NO$^-$) are not relevant from structural point of view and the two complexes show the same topology and very close bond parameters (see Tables S6 and S7 in the Supporting Information).

The neutral core of the centrosymmetric pentanuclear compound **5** can be described as a bowtie arrangement of five Ni^{II} ions, or, in other words, it is similar to two isosceles triangles sharing one vertex (Figure 1). Each triangle is μ_3−OH centered with the OH bridging group being displaced 0.725(2) Å out of the plane formed by the three Ni atoms. Two sides of the triangles are defined by single oximato bridges between the central and the peripheral nickel atoms whereas the external Ni^{II} atoms are bridged by one *syn*−*syn* acetate ligand and one $\mu_{1,1}$-N_3^- bridging group. Ni−N−Ni bond angle is 90.51(7)° and Ni−O−N−Ni torsion angles are quasiplanar (1.2(2)° and 3.4(2)°).

Central Ni(1) atom presents a NiO_6 environment that proceeds from the two μ_3-OH and four O-oximato ligands. Parallely, peripheral Ni(2,3) atoms exhibit a NiN_3O_3 environment that arises from one pyridyloxime ligand linked by its two N atoms, the μ-1,1 azide, the μ_3-OH central group, one *syn-syn* acetate ligand and finally one coordinated water molecule. Four intramolecular hydrogen bonds between the water molecules and the oxygen atom of the oximate groups help to stabilize the structure (Figure S5 in the Supporting Information). The crystallization water molecule establish intermolecular hydrogen bonds involving the coordinated water molecules giving a supramolecular 1D arrangement.

$\chi_M T$ vs. T plot for complexes **1**, **3**, and **5** are shown in Figure 2 (**3** and **4** show quasi identical bond parameters and **2** contains diamagnetic square planar nickel atoms and then, **2** and **4** were not measured). Complex **1** is ferromagnetically coupled; **3** shows an overall antiferromagnetic response whereas **5** exhibits the typical $\chi_M T$ minimum characteristic of ferrimagnetic behavior.

The experimental data was fitted according to the interaction patterns shown in Chart 2A for **1**, Chart 2B for **3**, Chart 2C for **5**, and the derived Hamiltonians:

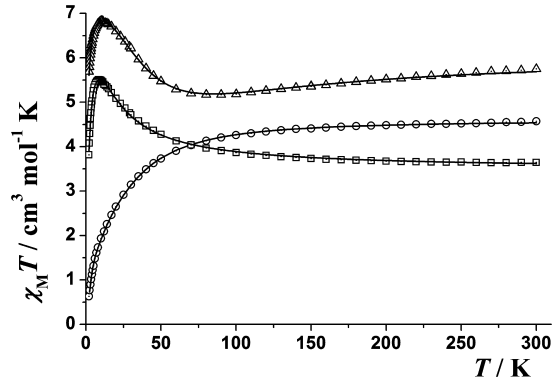

Figure 2. $\chi_M T$ vs T plot for complexes **1** (squares, □), **3** (circles, ○) and **5** (triangles, △). Solid lines show the best fit obtained.

Chart 2. Interaction Pattern with the Spin and Coupling Constant Labels for Topologies (A) 1, (B) 3, (C) 5, and (D) Metallacrowns 6 and 10[a]

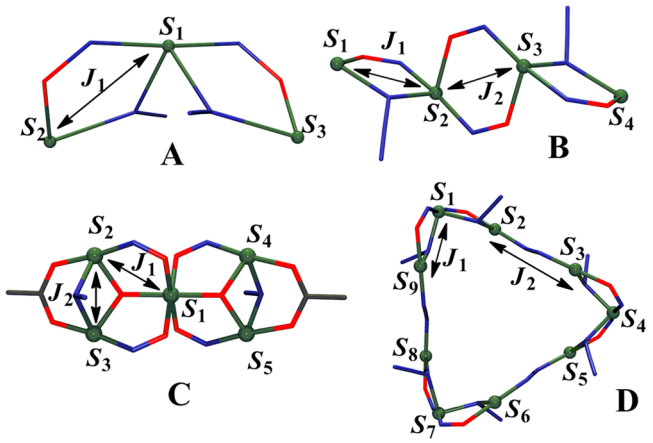

[a]See the text for the corresponding Hamiltonians.

$$H = -J_1(S_1 \cdot S_2 + S_1 \cdot S_3) \quad \text{for (1)}$$

$$H = -J_1(S_1 \cdot S_2 + S_3 \cdot S_4) - J_2(S_2 \cdot S_3) \quad \text{for (3)}$$

$$H = -J_1(S_1 \cdot S_2 + S_1 \cdot S_3 + S_1 \cdot S_4 + S_1 \cdot S_5) - J_2(S_2 \cdot S_3 + S_4 \cdot S_5) \quad \text{for (5)}$$

Compounds **1** and **5** were fitted with the derived analytical equations, whereas, for **3**, the CLUMAG program[19] was employed. Best-fit parameters were J_1 = +9.8(1) cm^{-1} and g = 2.155(3) for the trimeric complex **1**, J_1 = +10.2 cm^{-1}, J_2 = −28.7 cm^{-1}, g = 2.120 and $R = 3.56 \times 10^{-5}$ ($R = (\chi_M T_{exp} - \chi_M T_{calc})^2/(\chi_M T_{exp})^2$) for the tetranuclear complex **3** and J_1 = −24.3(1) cm^{-1}, J_2 = +23.1(4) cm^{-1} and g = 2.209(1) for the pentanuclear complex **5**.

The double oximato/μ-1,1-azide bridges between two Ni^{II} cations have been observed as fragments of larger clusters and overall ferromagnetic interaction was proposed for these fragments. However, complex **1** provides the unambiguous assignation of ferromagnetic coupling for this combination of superexchange pathways and it is confirmed by the value of J_1 obtained for complex **3**, which is in full agreement with **1**. From the sign and magnitude of the calculated coupling constants, the proposed ground states are S = 3 for **1**, S = 0 for **3**, and S = 3 for **5**.

dx.doi.org/10.1021/ic402651k | Inorg. Chem. 2014, 53, 1113−1121

Compounds **6**–**9**, and **12**, present the same structure except for the substitution pyC{ph}CNOH for py_2CNOH in **12** and the variation of the corresponding anion in each case. Thus, we only describe the structural details of **6** to avoid repetitive descriptions.

This compound can be described to be similar to three trimeric angular subunits linked by μ-1,3-azido bridges generating a $\{Ni_9\}$ ring, with Ni(1)–N(6)–Ni(2) bond angle of 110.89(7)° and Ni(1)–N(2)–O(1)–Ni(2) torsion angle of 17.6(2)°. Coordination of two oximate ligands to Ni(1) and the tridentate amines to Ni(2) are fully comparable with complex **1** and thus, the $\{Ni_9\}$ ring can be structurally described as a trimer of trimers (see Figure 3). The μ-1,3 bridges show Ni(2)–N(9)–N(10) bond angles of 128.2(2)° and a quasi planar Ni–NNN–Ni torsion angle of 171.8(1)°.

The shorter linkage sequence $\{-Ni-(\mu_{1,1}N_3)-Ni-(\mu_{1,1}N_3)-Ni-(\mu_{1,3}N_3)-\}_3$ determines a 24-membered ring containing six monatomic bridges (μ-1,1-azide) and three triatomic bridges (μ-1,3-azide), which gives the larger azido metallacrown reported to date.

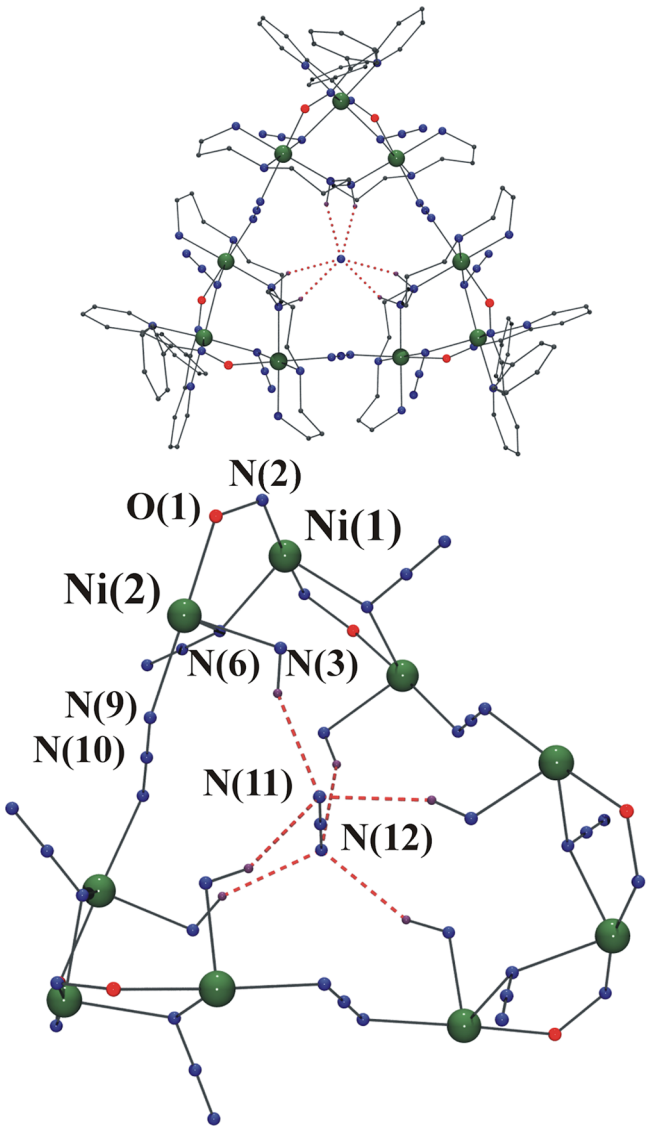

Figure 3. (Top) View of the molecular structure of complexes **6**–**9**, and **12**. (Bottom) Partially labeled core for all of them. Dashed bonds show the hydrogen bonds between the $-NH_2$ aminated functions and the coordinated azido guest.

The ring is not planar due to the arrangement of the μ-1,3-azido bridges, exhibiting a zig-zag ring conformation that generates a large internal prismatic cavity functionalized by six $-NH_2$ groups from the six dpt ligands (see Figure 4). These-NH_2 functions establish six hydrogen bonds with one azide anion trapped inside the cavity along the C_3 axis. N(3)–H(3a)···N(11) distance is 3.037(2) Å. In addition, a set of hydrogen bonds involving the N(6) atom from the μ-1,1-azide bridges and the aminated functions (N(3)–H(3b)···N(6), 3.117(2) Å and N(5)–H(5b)···N(6), 3.016(3) Å) helps to stabilize the *zig-zag* conformation of the ring. Relevant intermolecular interactions were not found.

Finally, the three positive charges on the ring are compensated by the guest azide anion and two ionic nitrates.

Compounds **10** and **11** exhibit the same metallacrown structure than the previous ones; however, in these cases, the $\{Ni_9\}$ rings encapsulate a bromide (**10**) or iodide (**11**) anion, also stabilized in this position by six hydrogen bonds. As in the above complexes **6**–**9**, and **12**, the cavity is a trigonal prism and the main bond parameters related with the bridging azide and oximato ligands are fully comparable, indicating that the conformation of the ring is poorly flexible (Figure 5). Detailed parameters for the hydrogen bonds are reported in Table S9 in the Supporting Information.

On basis of the common bond parameters in the bridging region for all the enneanuclear rings (Table 1), magnetic measurements were performed on a representative complex encapsulating one azide and one halide anion. $\chi_M T$ vs. T plot for complexes **6** and **10** are shown in Figure 6. Both of them exhibit a very similar shape and values indicating that, as should be expected, the guest anion does not influence the superexchange interactions.

The experimental data was fitted with the CLUMAG program,[19] according to the interaction pattern shown in Chart 2D and the derived Hamiltonian:

$$H = -J_1(S_9 \cdot S_1 + S_1 \cdot S_2 + S_3 \cdot S_4 + S_4 \cdot S_5 + S_6 \cdot S_7 + S_7 \cdot S_8) - J_2(S_2 \cdot S_3 + S_5 \cdot S_6 + S_8 \cdot S_9)$$

Best-fit parameters were $J_1 = +9.9\ cm^{-1}$, $J_2 = -62.5\ cm^{-1}$, $g = 2.289$, and $R = 1.25 \times 10^{-5}$ for **6** and $J_1 = +8.9\ cm^{-1}$, $J_2 = -53.5\ cm^{-1}$, $g = 2.211$, and $R = 1.57 \times 10^{-5}$ for **10**.

As expected from the similar bond parameters of the double oximato/μ-1,1-azide bridges, J_1 gives very close values to complexes **1** and **3**. The sign and magnitude of J_2 is indicative of strong antiferromagnetic coupling, which lies in the expected range[20] of values for a single μ-1,3-azido bridge with torsion angles of ~175° and Ni–N–N bond angles close to 129°. The lower AF interaction for **10** can be attributed to the larger Ni–N bond distance.

It should be emphasized that the coupling constants $(-J_1 - J_1 - J_2)_3$ alternating with ferromagnetic J_1 and antiferromagnetic J_2 in a closed ring is unusual from a magnetic point of view. The strong AF interaction J_2 cancels three pairs of spins but remain three $S = 1$ corners leading to a situation similar to a Ni^{II} triangle with diamagnetic $S = 0$ ground state, despite the odd number of spins (see Figure S6 in the Supporting Information).

Host–Guest Interactions. Synthesis by self-assembly of the metallacrowns **6**–**12** is the result of the subtle combination of several factors as charge balance, anionic effects, guest

dx.doi.org/10.1021/ic402651k | Inorg. Chem. 2014, 53, 1113–1121

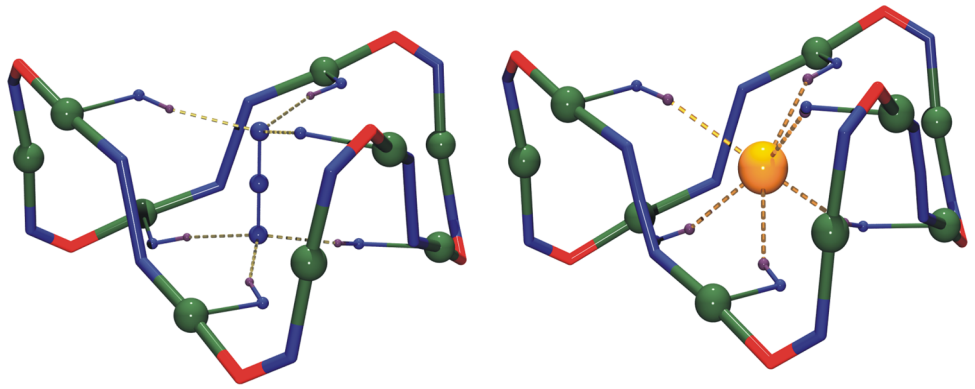

Figure 4. View of the *zig-zag* conformation of the ring and the prismatic cavity hosting the azide anion for compounds **6**–**9** as **12** (left), and compounds **10** and **11** (right).

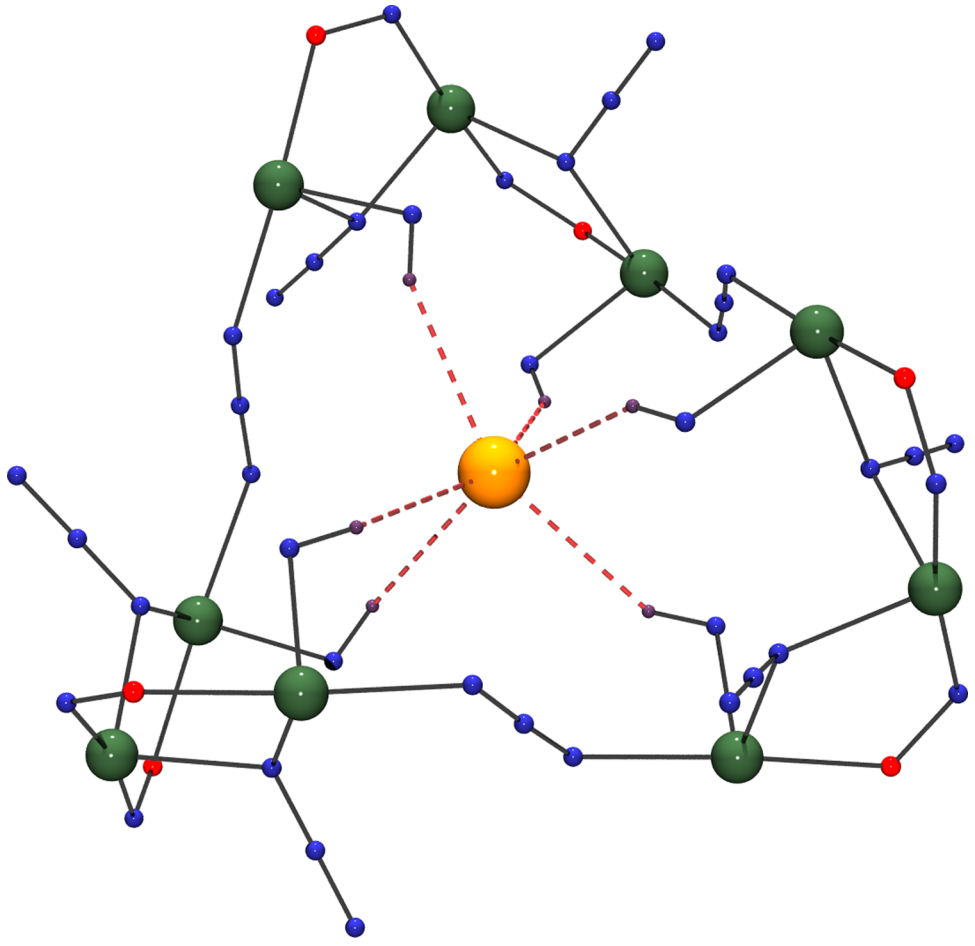

Figure 5. View of the metallacrown and the set of hydrogen bonds (dashed bonds) that coordinate the halide guests in compounds **10** and **11**. Atom labeling is the same as that for compounds **6**–**9**, and **12**.

coordination and hydrogen-bond interactions, which lead to the stabilization of this unusual supramolecular system. The detailed analysis of these factors will be the subject of this section.

Anion Effect. The reaction of Ni^{II}, tridentate amines, and 2-pyridyloximes without other anions in the reaction medium than azido or oximate lead to neutral low nuclearity systems (Ni_3, Ni_4), which contain the nickel centers bonded by double azido/oximato bridges. In contrast, the presence in the reaction medium of a large variety of anions stabilizes the cationic nonanuclear metallacronws **6**–**12** independently of the shape or size of the anions (NO_3^-, BF_4^-, ClO_4^-, F^-, Cl^-, Br^-, I^-). The structure of the metallacrowns **6**–**12** shows an evident relationship with trimeric complex **1** and they can be described as "trimers of trimers", which are linked by μ-1,3-azido bridges. Two factors emerge as driving force for these reactions: on one hand, counteranions are necessary to balance the positive charge of the ring, and on the other hand, the reaction needs a small anion (azide or halide) to give a template assembly around it. The anionic guest and the counteranion become equally crucial to determine the stability and topology of the enneanuclear metallacrowns.

dx.doi.org/10.1021/ic402651k | *Inorg. Chem.* 2014, 53, 1113–1121

Table 1. Selected Interatomic Angles Related with the Azido Bridges and Oximate Torsion for Compounds 6−12

	Interatomic Angles (deg)		
compound	Ni(1)−N(6)−Ni(2)	Ni(2)−N(9)−N(10)	Ni(1)−N(2)−O(1)−Ni(2)
6	110.89(7)	128.2(2)	17.6(2)
7	110.8(1)	127.6(2)	17.6(3)
8	110.9(1)	127.9(3)	17.3(4)
9	111.1(1)	130.0(2)	14.8(4)
10	111.0(1)	129.2(3)	15.2(4)
11	111.3(2)	129.7(4)	17.8(5)
12	111.1(1)	127.0(2)	18.6(4)

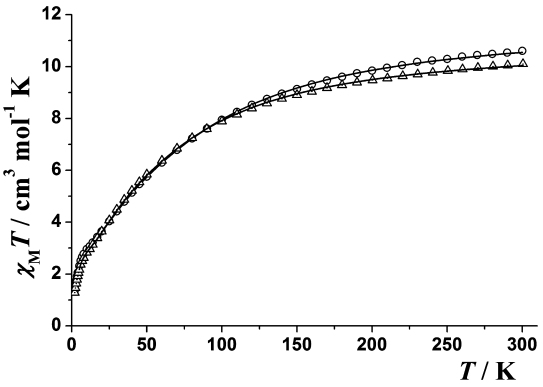

Figure 6. $\chi_M T$ vs T plot for complexes **6** (circles) and **10** (triangles). Solid lines show the best fit obtained.

Scheme 1. *Stoichiometric* Relationship between Complex 1 and Complexes 6−9, as Well as 12

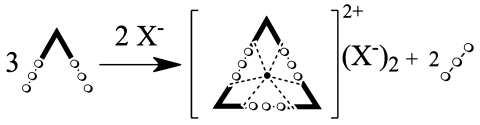

Although Scheme 1 does not correspond to one real reaction, it illustrates the "*stoichiometric*" relationship and the anion role between trinuclear complex **1** and enneanuclear complexes **6−9**, and **12**, which contain one azide as an anionic guest.

Azide as a Guest. Compounds **6−9**, and **12**, coordinate the guest azide in a manner similar to that of Lehn's [BT-6H$^+$] cryptand[6] (trigonal prismatic arrangement). This arrangement arises from six hydrogen bonds established between six $-NH_2$ amino functions of the dpt ligands. The trigonal prisms and even their distortions are surprisingly similar between the cryptand and the {Ni$_9$} rings, being the main difference the degree of pyramidalization of the hydrogen bonds, which determines the bases of the prisms (see Chart 3 and Table 2).

Table 2. Comparison between [BT-6H$^+$] and {Ni$_9$} Prism Parameters

compound	H^a	T	S	D^b	N−N$_{az}$−N (deg)	N−H···N
6	3.933	5.022	4.013	3.552	114.98	3.037
7	3.940	5.096	4.023	3.541	113.49	3.047
8	3.954	5.149	4.025	3.570	113.23	3.083
9	3.876	5.136	3.949	3.542	114.23	3.058
12	3.994	5.086	4.064	3.551	113.12	3.048
A^c	5.396	4.364	5.528	3.693	95.03	2.959
10	3.786	5.176	3.861	3.538		
11	3.922	5.207	4.013	3.590		
B^{d,e}	4.226	4.580	4.922	3.390		

^{a}Polyhedron height measured as the distance between the centroids of the opposite triangular faces. ^{b}Distance from the N-donor atoms to the centroid of the cavity. ^{c}**A** = (N_3) ⊂ [BT-6H$^+$]. ^{d}**B** = (Br) ⊂ [BT-6H$^+$]. ^{e}Average values.

Analysis of the above data points out that the prismatic cavity is practically identical in all **6−12** cases. Comparison with compound **A** shows that, although the cavity is clearly compressed in complexes **6−9**, and **12**, the N−H···N distances serve as evidence that the hydrogen bonds are equally effective in the cryptand than in the {Ni$_9$} metallacrowns.

Halides as Guest. The [BT-6H$^+$] cryptand is able to coordinate azido anions but also spherical anions as halides. The highly flexible cryptand can rearrange its conformation by rotation in opposite sense of their two moieties along its main edge and then generate an octahedral environment that fits spherical guests more adequately.[6] The reported {Ni$_9$} metallacrown is much more rigid and unable to change its conformation.

Chart 3. Prismatic Coordination of the Anionic Guests in (A) (N_3) ⊂ [BT-6H$^+$] Cryptand, (B) Compounds 6−9 and 12, and (C) 10 and 11 (the Image to the Far Right Describes the Structural Parameters Summarized in Table 2)^a

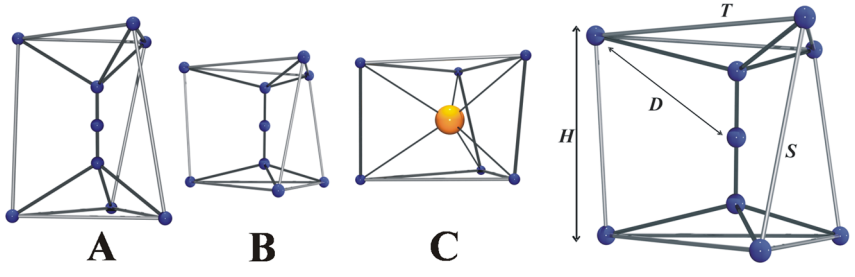

^{a}All distances refer to positions of the N atoms involved in the six hydrogen bonds.

dx.doi.org/10.1021/ic402651k | *Inorg. Chem.* 2014, 53, 1113−1121

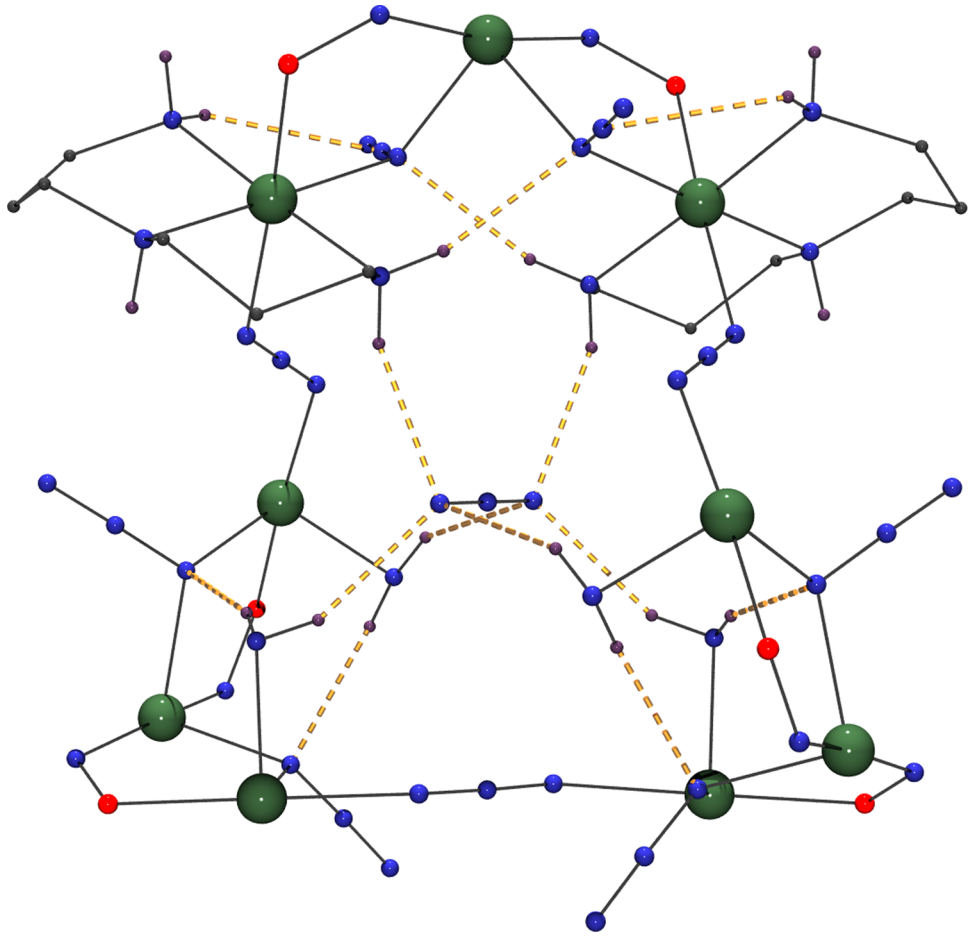

Figure 7. Set of hydrogen bonds promoted by the $-NH_2$ functions in **6**−**12**.

However, the compressed prisms **6**−**9**, and **12**, show distances to the centroid of the cavity that are only slightly larger than those found in (Br)[BT-6H$^+$] (see Table 2), suggesting that halides could fit into these prismatic cavities. This possibility was explored and complexes **10** and **11**, containing one bromide and one iodide guest in the unprecedented prismatic trigonal coordination (see Chart 3) were successfully characterized showing that the shape of the cavity is not a determinant factor. In contrast, reactions with nickel fluoride or chloride yielded the above-described complexes **8** and **9** in which the smaller halides act only as counteranions and the cavity is occupied by one guest azide, evidencing that the main factor involved with encapsulating the halides is their size.

Tridentate Amines Role. The tridentate aminated ligands establish a pack of six hydrogen bonds with both central azide and halide guest anions, but the role of these ligands can be considered not only to trap the central anion, but also to stabilize the {Ni$_9$} ring. As it can be seen in Figure 7, the $-NH_2$ functions pointing to the center of the cavity link the guest anion with one of their H atoms, whereas they establish another hydrogen bond employing their second H atom with the N(6) atom of the μ-1,1-azido ligand. N(6) is also the receptor of a second hydrogen bond from the $-NH_2$ function in *trans* to the inner $-NH_2$ group. Thus, the *mer* coordination of the ligand becomes essential to stabilize the entire ring, pointing out that dpt is the optimal choice to generate these types of rings.

As experimental proof, the change of dpt ligand by *N*,*N*′,*N*″-Me$_3$dpt, which is unable to establish some of the hydrogen-bond interactions, stabilizes complex **4** instead of the {Ni$_9$} ring. Equally, experiments trying the substitution of the dpt tridentate amine by the bidentate *N*-Meen (*N*-methylethylenediamine), capable of establishing hydrogen-bond interactions with the central anion host but not with the nearby μ-1,1-azide ligands leads to completely different topologies and nuclearities.[10c]

Selectivity. One should remember that these complexes are not stable in solution and the selectivity considerations concern the complexes in solid state exclusively. As has been proven, the {Ni$_9$} ring is able to encapsulate one azide/halide anion. However, it is noteworthy that, in all reactions involving **6**−**12**, there exists a competition between the azide, which is always present in the reaction medium, and the corresponding Ni^{2+} counterion (NO_3^-, BF_4^-, ClO_4^-, or the halides) to fill the guest site. Tetrahedral anions as BF_4^- or ClO_4^- can coordinate in prismatic environments but they require larger cavities to fit adequately,[21] and their inclusion in the {Ni$_9$} cavity should be discarded as well for the smaller halides (F, Cl^-) for which the rigid cavity is too large to give effective hydrogen bonds. Thus, experimental results indicate that the encapsulation inside the {Ni$_9$} metallacrown is controlled by the size of the cavity and that Br^- and I^- ions are preferred to the N_3^- species.

dx.doi.org/10.1021/ic402651k | *Inorg. Chem.* 2014, 53, 1113−1121

CONCLUSIONS

Tridentate amines and 2-pyridyloximate blend of ligands have been demonstrated to be adequate for the syntheses of new and unprecedented topologies in oximato chemistry, such as compound **1**, which provided unambiguous experimental evidence of the ferromagnetic interaction promoted by double oximate/azide bridges. Also, a series of Ni_3, Ni_4, and Ni_5 complexes have been synthesized, as well as a family of self-assembled cryptand-like $\{Ni_9\}$ rings that are able to selectively encapsulate azide/halide anions, by reaction of different Ni^{2+} salts, azide, and dipyridylketoneoximate or phenylpyridylketoneoximate ligands.

The azide/halide coordination takes place around six hydrogen bonds and generates a quiral helical arrangement of the cavity of the $\{Ni_9\}$ ring. N_3^-, Br^-, and I^- adequately fit the cavity size, excluding other larger or smaller anions. The *mer* coordination of the aminated tridentate ligand determines the stabilization of the $\{Ni_9\}$ rings by means of a set of additional hydrogen bonds involving the two $-NH_2$ functions.

ASSOCIATED CONTENT

Supporting Information

Crystallographic data (CIF format), synthetic details, crystallographic information for compounds **1**−**12**, and Ni_9 ring spin levels energy diagram. This material is available free of charge via the Internet at http://pubs.acs.org.

AUTHOR INFORMATION

Corresponding Author

*E-mail: albert.escuer@qi.ub.es.

Notes

The authors declare no competing financial interests.

ACKNOWLEDGMENTS

Funding from the CICYT (Project No. CTQ2012-30662) are acknowledged. A.E. is thankful for financial support from the Excellence in Research ICREA-Academia Award.

REFERENCES

(1) (a) Gale, P. A.; Gunnlaugsson, T. *Chem. Soc. Rev.* **2010**, *39*, 3595. (b) Steed, J. *Chem. Soc. Rev.* **2009**, *38*, 506. (c) Sessler, J. L.; Gale, P. A.; Cho, W.-S. *Anion Receptor Chemistry*; Royal Society of Chemistry: Cambridge, U.K., 2006. (d) Kang, S. O.; Begum, R. A.; Bowman-James, K. *Angew. Chem., Int. Ed.* **2006**, *45*, 7882. (e) Bowman-James, K. *Acc. Chem. Res.* **2005**, *38*, 671.

(2) (a) Ballester, P. *Chem. Soc. Rev.* **2010**, *39*, 3810. (b) Lawrance, G. A. *Chem. Rev.* **1986**, *86*, 17. (c) Saalfrank, R. W.; Demleitner, B.; Glaser, H.; Maid, H.; Bathelt, D.; Hampel, F.; Bauer, W.; Teichert, M. *Chem.—Eur. J.* **2002**, *8*, 2679. (d) Albrecht, M.; Janser, I.; Meyer, S.; Weis, P.; Frohlich, R. *Chem. Commun.* **2003**, 2854. (e) Glasson, C. R. K.; Meehan, G. V.; Clegg, J. K.; Lindoy, L. F.; Turner, P.; Duriska, M. B.; Willis, R. *Chem. Commun.* **2008**, 1190. (f) Custelcean, R.; Bosano, J.; Bonnesen, P. V.; Kertesz, V.; Hay, B. P. *Angew. Chem., Int. Ed.* **2009**, *48*, 4025. (g) Bryantsev, V. S.; Hay, B. P. *J. Am. Chem. Soc.* **2006**, *128*, 2035.

(3) Diederich, F., Slang, P. J., Eds. *Templated Organic Synthesis*; Wiley−VCH: Weinheim, Germany, 2000.

(4) Kang, S. O.; Llinares, J. M.; Day, V. W.; Bowman-James, K. *Chem. Soc. Rev.* **2010**, *39*, 3980.

(5) (a) Beer, P. D.; Gale, P. A. *Angew. Chem., Int. Ed.* **2001**, *40*, 486. (b) Rice, C. R. *Coord. Chem. Rev.* **2006**, *250*, 3190. (c) Pérez, J.; Riera, L. *Chem. Soc. Rev.* **2008**, *37*, 2658. (d) Fabbrizzi, L.; Poggi, A. *Chem. Soc. Rev.* **2013**, *42*, 1861.

(6) Dietrich, B.; Guilhem, J.; Lehn, J. M.; Pascard, C.; Sonveaux, E. *Helvet. Chim. Acta* **1984**, *67*, 91.

(7) (a) Kim, N.-K.; Chang, K.-J.; Moon, D.; Lah, M. S.; Jeong, K.-S. *Chem. Commun.* **2007**, 3401. (b) Kang, S. O.; Day, V. W.; Bowman-James, K. *Inorg. Chem.* **2010**, *49*, 8629. (c) Serpell, C. J.; Cookson, J.; Thompson, A. L.; Beer, P. D. *Chem. Sci.* **2011**, *2*, 494. (d) Wang, X.; Jia, C.; Huang, X.; Wu, B. *Inorg. Chem. Commun.* **2011**, *14*, 1508. (e) Bushmarinov, I. S.; Nabiev, O. G.; Kostyanovsky, R. G.; Antipina, M. Y.; Lyssenko, K. A. *Cryst. Eng. Commun.* **2011**, *13*, 2930.

(8) Amendola, V.; Boiocchi, M.; Colasson, B.; Fabbrizzi, L.; Rodriguez-Douton, M. J.; Ugozzoli, F. *Angew. Chem., Int. Ed.* **2006**, *45*, 6920.

(9) (a) Milios, C. J.; Stamatatos, T. C.; Perlepes, S. P. *Polyhedron* **2006**, *25*, 134. (b) Tasiopoulos, A. J.; Perlepes, S. P. *Dalton Trans.* **2008**, 5537.

(10) (a) Stamatatos, T. C.; Abboud, K. A.; Perlepes, S. P.; Christou, G. *Dalton Trans.* **2007**, 3861. (b) Stamatatos, T. C.; Escuer, A.; Abboud, K. A.; Raptopoulou, C. P.; Perlepes, S. P.; Christou, G. *Inorg. Chem.* **2008**, *47*, 11825. (c) Esteban, J.; Alcazar, L.; Torres-Molina, M.; Monfort, M.; Font-Bardia, M.; Escuer, A. *Inorg. Chem.* **2012**, *51*, 5503.

(11) Papatriantafyllopoulou, C.; Stamatatos, T. C.; Wernsdorfer, W.; Teat, S. J.; Tasiopoulos, A. J.; Escuer, A.; Perlepes, S. P. *Inorg. Chem.* **2010**, *49*, 10486.

(12) Escuer, A.; Esteban, J.; Font-Bardia, M. *Chem. Commun.* **2012**, *48*, 9777.

(13) Sheldrick, G. M. *SHELXS—A Computer Program for Determination of Crystal Structures*; University of Göttingen: Göttingen, Germany, 1997.

(14) Sheldrick, G. M. *SHELX97—A Computer Program for Determination of Crystal Structures*; University of Göttingen: Göttingen, Germany, 1997.

(15) Farrugia, L. J. *J. Appl. Crystallogr.* **1997**, *30*, 565 (Ortep-3 for Windows).

(16) Escuer, A.; Vicente, R.; Ribas, J.; Solans, X. *Inorg. Chem.* **1995**, *34*, 1793.

(17) Esteban, J.; Ruiz, E.; Font-Bardia, M.; Calvet, T.; Escuer, A. *Chem.—Eur. J.* **2012**, *18*, 3637.

(18) (a) Escuer, A.; Esteban, J.; Aliaga-Alcalde, N.; Font-Bardia, M.; Calvet, T.; Roubeau, O.; Teat, S. J. *Inorg. Chem.* **2010**, *39*, 2259. (b) Escuer, A.; Esteban, J.; Roubeau, O. *Inorg. Chem.* **2011**, *50*, 8893. (c) Esteban, J.; Escuer, A.; Font-Bardia, M.; Roubeau, O.; Teat, S. J. *Polyhedron* **2013**, *52*, 339.

(19) Gatteschi, D.; Pardi, L. *Gazz. Chim. Ital.* **1993**, *123*, 231 (CLUMAG program).

(20) Escuer, A.; Vicente, R.; Ribas, J.; El Fallah, M. S.; Solans, X.; Font-Bardia, M. *Inorg. Chem.* **1994**, *33*, 1842.

(21) Paul, R. L.; Bell, Z. R.; Jeffery, J. C.; McCleverty, J. A.; Ward, M. D. *Proc. Natl. Acad. Sci. U.S.A.* **2002**, *99*, 4883.